XUN LI

Optoelectronic Devices

Design, Modeling, and Simulation

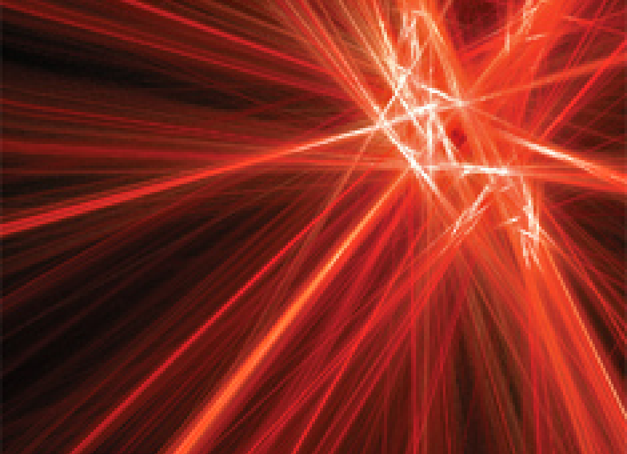

CAMBRIDGE

CAMBRIDGE www.cambridge.org/9780521875103

This page intentionally left blank

Optoelectronic Devices

Design, Modeling, and Simulation

With a clear application focus, this book explores optoelectronic device design and modeling through physics models and systematic numerical analysis.

By obtaining solutions directly from the physics-based governing equations through numerical techniques, the author shows how to design new devices and how to enhance the performance of existing devices. Semiconductor-based optoelectronic devices such as semiconductor laser diodes, electro-absorption modulators, semiconductor optical amplifiers, superluminescent light-emitting diodes and their integrations are all covered.

Including step-by-step practical design and simulation examples, together with detailed numerical algorithms, this book provides researchers, device designers, and graduate students in optoelectronics with the numerical techniques to solve their own structures.

Xun Li is a Professor in the Department of Electrical and Computer Engineering at McMaster University, Hamilton. Since receiving his Ph.D. from Beijing Jiaotong University in 1988, he has authored and co-authored over 160 technical papers and co-founded Apollo Photonics, Inc., developing one of the company's major software products, "Advanced Laser Diode Simulator". He is a Member of the OSA and SPIE, and a Senior Member of the IEEE.

Optoelectronic Devices

Design, Modeling, and Simulation

XUN LI

Department of Electrical and Computer Engineering
McMaster University
Hamilton, Ontario

CAMBRIDGE UNIVERSITY PRESS

CAMBRIDGE UNIVERSITY PRESS
Cambridge, New York, Melbourne, Madrid, Cape Town, Singapore,
São Paulo, Delhi, Dubai, Tokyo

Cambridge University Press
The Edinburgh Building, Cambridge CB2 8RU, UK

Published in the United States of America by Cambridge University Press, New York

www.cambridge.org
Information on this title: www.cambridge.org/9780521875103

First published in print format 2009

ISBN-13 978-0-511-57749-9 eBook (Adobe Reader)

ISBN-13 978-0-521-87510-3 Hardback

Contents

Preface

Over the past 30 years, the world has witnessed the rapid development of optoelectronic devices based on III-V compound semiconductors. Past effort has mainly been directed to the theoretical understanding of, and the technology development for, these devices in applications in telecommunication networks and compact disk (CD) data storage. With the growing deployment of such devices in new fields such as illumination, display, fiber sensor, fiber gyro, optical coherent tomography, etc., research on optoelectronic devices, especially on those light emitting components, continues to expand with the pursuit of many experimental explorations on new materials such as group-III nitride alloys and II-VI compounds and novel structures such as quantum wires, dots, and nanostructures.

As the manufacturing technology becomes mature and standardized and few uncertainties are left, design and simulation become the major issue in the performance enhancement of existing devices and in the development of new devices. Recent progress in numerical techniques as well as computing hardware has provided a powerful platform that makes sophisticated computer-aided design, modeling, and simulation possible. So far, the development of optoelectronic devices seems to replicate the history of electronic devices: from discrete to integrated, from technology intensive to design intensive, from trial-and-error experiments to computer-aided simulation and optimization.

The purpose of this book is to bridge the gap between the theoretical framework and the solution to real-world problems, or, more specifically, to bridge the gap between our knowledge acquired on electromagnetic field theory, quantum mechanics, and semiconductor physics and optoelectronic device design and modeling through advanced numerical tools.

Advanced optoelectronic devices are built on compound semiconductor material systems with complicated geometrical structures; they are also operated under varying conditions. For this reason, we can find hardly any easy, intuitive, and analytical solutions to the first-principle-based governing equations that accurately describe the closely coupled physical processes inside such devices. Although solutions are relatively easy to obtain from the equations derived from the phenomenological model, assumptions have to be made in such a model, which often ignores some important effects and fails to achieve quantitative agreement between theoretically predicted and practically measured results.

Therefore, obtaining the solution directly from the physics-based governing equations through numerical techniques seems to be a promising approach to bridge the gap as mentioned above, as not only a qualitative, but also a quantitative matching between the theory and experiment is achievable. This book is intended for readers who want to link their understanding of the device physics through the theoretical framework they have already acquired to the design, modeling and simulation of real-world devices and innovative structures.

This book will focus on semiconductor-based optoelectronic devices such as laser diodes (LDs), electro-absorption modulators (EAMs), semiconductor optical amplifiers (SOAs), and superluminescent light emitting diodes (SLEDs) in various applications. Numerical methods will be used throughout the analysis of these devices.

Derived from physics-based first principles, governing equations will be given for the description of different physical processes, such as light propagation, optical gain generation, carrier transport and thermal diffusion, and their interplays inside the devices. Different numerical techniques will be discussed in detail along with the process of seeking the solution to these governing equations. Discussions on device design optimizations will also be followed, based on the interpretation of the numerical solutions.

The methodology introduced in this book hopefully will help its readers to learn (1) how to extract the governing equations from first principles for the accurate description of their devices; and more importantly, (2) how to obtain the numerical solution to those governing equations once derived. Practical design and simulation examples are also given to support the approaches used in this book.

I am in debt to my colleague and friend, Professor W.-P. Huang, who showed me the prospect of computer-aided design, modeling and simulation in this field 15 years ago, and with whom I had countless stimulating discussions on almost every topic involved in this book, from the material physics to waveguide theory, from the model establishment to result interpretation, and from the modeling methodology to numerical algorithm. I would like to thank Dr. T. Makino (former Nortel), Dr. K. Yokoyama (former NTT), Dr. T. Yamanaka (NTT), Dr. C.-L. Xu (RSoft Inc.), Dr. J. Hong (Oplink Inc.), Dr. A. Shams (former Photonami Inc.), Professor S. Sadeghi (University of Alabama at Huntsville), Professor W. Li (University of Wisconsin at Platteville), Professor Y. Luo (Tsinghua University), Professor Y.-H. Zhang (Arizona State University), Ms. T.-N. Li (InPhenix Inc.), Ms. N. Zhou (AcceLink Co.), Mr. M. Mazed (IP Photonics Inc.), Professor T. Luo (University of Minnesota), Professor C.-Q. Xu (McMaster University), Professor M. Dagenais (University of Maryland at College Park), Dr. J. Piprek (former University of California at Santa Barbara), and many other colleagues and friends in this field, for numerous insightful and inspiring discussions and interactions on various subjects in this book, during and after our research collaborations. I am grateful to Ms. Y.-P. Xi, who helped me with the simulation of SOAs and SLEDs, and Mr. Q.-Y. Xu, who helped me with the simulation of crosstalks in the integrated DFB laser and monitoring photodetector. I am also grateful to Professor S.-H. Chen (Huazhong University of Sci. and Tech.) and her graduate students, who helped me to create most of the schematic diagrams in the first eight chapters and all the three-dimensional device structure drawings in Chapters 10 and 12. I would also like to thank my graduate students and many other graduate students in the Department of Electrical and Computer Engineering at McMaster University who took my course on this subject, for their valuable comments and suggestions. Finally, I appreciate the constant help and great patience of Dr. J. Lancashire and Ms. S. Koch.

1 Introduction

1.1 The underlying physics in device operation

Figure 1.1 shows the major physical processes and their linkages in the operation of optoelectronic devices.

To capture these physical processes, we need the following models and knowledge:

(1) a model that describes wave propagation along the device waveguide (electromagnetic wave theory);
(2) a model that describes the optical properties of the device material platform (semiconductor physics);
(3) a model that describes carrier transport inside the device (quasi-electrostatic theory);
(4) a model that describes thermal diffusion inside the device (thermal diffusion theory).

Therefore, the above four aspects should be included in any model established for simulation of optoelectronic devices.

1.2 Modeling and simulation methodologies

There are two major approaches in device modeling and simulation.

(1) Physics modeling: a direct approach based on the first principle physics-based model.

The required governing equations in the preceding four aspects are all derived from first principles, such as the Maxwell equations (including electromagnetic wave theory for the optical field distribution and quasi-electrostatic theory for the carrier transport), the Schrödinger equation (for the semiconductor band structure), the Heisenberg equation (for the gain and refractive index change), and the thermal diffusion equation (for the temperature distribution).

This model gives the physical description of what exactly happens inside the device and is capable of providing predictions on device performance in every aspect, once the device building material constants, the structural geometrical sizes, and the operating conditions are all given.

This approach is usually adopted by device designers who work on developing devices themselves.

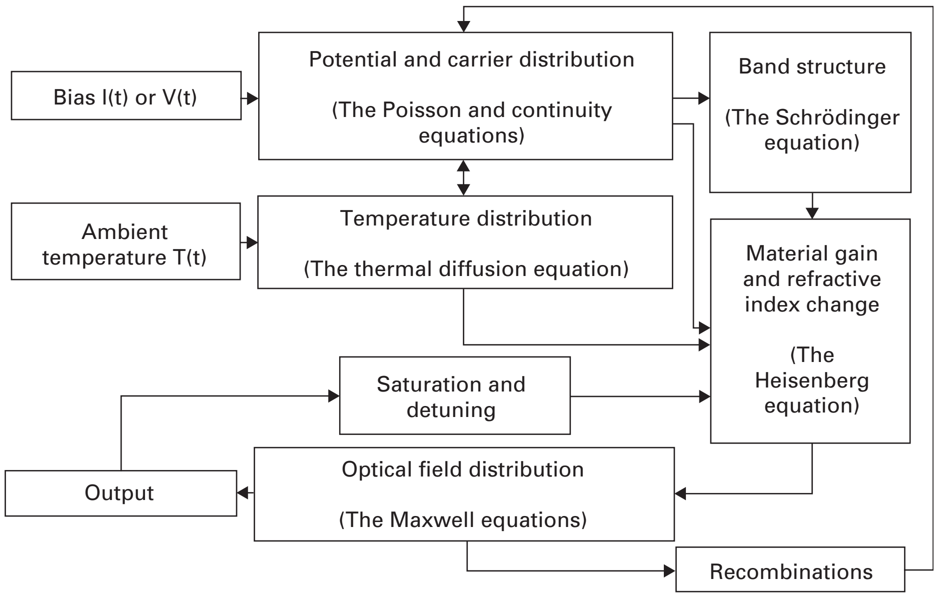

Fig. 1.1. The physical processes and their linkages in the operation of optoelectronic devices. Noted in brackets are the first principle equations that govern these processes.

However, such a modeling technique is usually complex and sophisticated numerical tools have to be invoked in solving the equations involved. Computationally it is usually expensive.

(2) Behavior modeling: an indirect approach based on an equivalent or phenomenological model.

The governing equations in the preceding four aspects are extracted from first principles under various assumptions. Hence they are greatly simplified compared with the equations in the physics-based model. Those frequently used methods in the extraction of the simplified equations include: (1) reducing or even eliminating spatial dimensions; (2) neglecting the dependence that causes only relatively slow or small variation; and (3) ignoring the physical processes that have little direct effect on the aspects of interest. Another method is to replace the original local or discrete variable by a global or integrated variable in the description of the physical process, as the latter usually obeys a certain conservation law, hence a corresponding balance equation can be derived in a simple form.

This model does not give the description of what exactly happens inside the device but is capable of providing the same device terminal performance as the physics-based model. Therefore, if the device is treated as a black box, this model will provide the correct output for any given input.

This approach is usually adopted by circuit and system designers who just use rather than develop devices.

Although this modeling technique is usually simple and computationally inexpensive, it has two major drawbacks that prevent its application in device design and development. The first demerit is that it can give hardly any physical insights. Little information can be obtained on how to make a device work better by improving the design. The second demerit is that it often relies on non-physical input parameters, such as effective constants or phenomenologically introduced coefficients, which are usually difficult to obtain.

In optoelectronic device modeling, we normally take a combination of the preceding two approaches. Depending on different simulation requirements, we usually retain a minimum set of the necessary physics-based equations and replace the rest by simplified ones.

1.3 Device modeling aspects

In device modeling, we normally look at the following aspects.

(1) Device steady state performance.
No time dependence needs to be considered in this simulation. The device characteristics are usually modeled as functions of the bias.
(2) Device small-signal dynamic performance.
Based on the small-signal linearization, a direct current (DC) at a fixed bias plus a frequency domain analysis are required in this simulation.
(3) Device large-signal dynamic performance.
A direct time-domain analysis is required in the simulation.
(4) Noise performance.
Either a semi-analytical frequency domain analysis or a numerical time-domain analysis is required in this simulation.

1.4 Device modeling techniques

A typical procedure for optoelectronic device modeling and simulation includes:

(1) input geometrical structures;
(2) input material constants;
(3) set up meshes;
(4) initialize solvers (pre-processing);
(5) input operating conditions;
(6) scale variables (physical to numerical);
(7) start looping;
(8) call carrier solver;
(9) call temperature solver;
(10) call material solver;
(11) call optical solver;

(12) go back to step 7 until convergence;
(13) scale variables (numerical to physical);
(14) output assembly (post-processing).

To start this procedure, however, one must have an initial device structure, which relies on one's understanding of the device physics and on one's experience accumulated from analysis and interpretation of the results obtained from device design, modeling and simulation practice.

Other than the initial structure, we still need to collect all the input parameters required by the numerical solvers. These parameters are usually obtained from open literature, experiment, or calibration.

The following are a number of numerical techniques that are often involved in optoelectronic device modeling:

(1) partial differential equation (PDE) solvers (boundary value and mixed boundary and initial value problems);
(2) ordinary differential equation (ODE) solvers (initial and boundary value problems);
(3) algebraic eigenvalue problem solvers;
(4) linear and non-linear system of algebraic equations solvers;
(5) root searching routine;
(6) minimization or maximization routine;
(7) function evaluations, interpolation and extrapolation routines;
(8) numerical quadratures;
(9) fast Fourier transform (FFT) and digital filtering routines;
(10) pseudo-random number generation.

The key issue in device modeling is to establish numerical solvers for PDEs, which usually follows a procedure as shown below.

(1) Scale the variables in given PDEs.
(2) Set up computation window and mesh grids.

(These two steps translate a physical problem into a numerical problem.)

(3) Equation discretization through, e.g., finite difference (FD) scheme.
(4) Boundary processing.

(These two steps translate PDEs into a system of algebraic equations.)

(5) Start Newton's iteration for the system of non-linear algebraic equations.

(This step translates the system of non-linear algebraic equations into a system of linear algebraic equations.)

(6) Find solution to the system of linear algebraic equations.
    Direct method (for moderate size or dense coefficient matrix).
    Iterative method (for large size sparse coefficient matrix).
    Convergence acceleration (for iterative method).

(7) Convergence acceleration for Newton's iteration.

(The numerical solution will be obtained after this step.)

(8) Scale variables and post processing.

(A physical solution will be obtained after this step.)

1.5 Overview

This book is divided into three parts. The first part, comprising Chapters 2, 3, 4, and 5, is on the derivation and explanation of governing equations that model the closely coupled physics processes in optoelectronic devices. The second part, Chapters 6, 7, 8, and 9, is devoted to numerical solution techniques for the governing equations arising from the first part and explains how these techniques are jointly applied in device simulation. Chapters 10, 11, and 12 form the third part, which provides real-world design and simulation examples of optoelectronic devices, such as Fabry–Perot (FP) and distributed feedback (DFB) LDs, EAMs, SOAs, SLEDs, and their monolithic integrations.

2 Optical models

2.1 The wave equation in active media

2.1.1 Maxwell equations

The behavior of the optical wave is generally governed by the Maxwell equations

$$\nabla \times \vec{E}(\vec{r}, t) = -\frac{\partial}{\partial t}\vec{B}(\vec{r}, t), \tag{2.1}$$

$$\nabla \times \vec{H}(\vec{r}, t) = \frac{\partial}{\partial t}\vec{D}(\vec{r}, t) + \vec{J}(\vec{r}, t), \tag{2.2}$$

$$\nabla \cdot \vec{D}(\vec{r}, t) = \rho(\vec{r}, t), \tag{2.3}$$

$$\nabla \cdot \vec{B}(\vec{r}, t) = 0, \tag{2.4}$$

where $\vec{E}$ and $\vec{H}$ indicate the electric and magnetic fields in V/m and A/m, respectively, r and t represent the space coordinate vector and time variable, respectively, $\vec{D}$ the electric flux density in C/m^2, $\vec{B}$ the magnetic flux density in Wb/m^2, $\vec{J}$ the current density in A/m^2, and ρ the charge density in C/m^3.

In semiconductors, the constitutive relation reads

$$\vec{D}(\vec{r}, t) = \int_{-\infty}^{t} \varepsilon(\vec{r}, t-\tau)\vec{E}(\vec{r}, \tau)\mathrm{d}\tau, \tag{2.5}$$

$$\vec{B}(\vec{r}, t) = \mu_0 \vec{H}(\vec{r}, \tau), \tag{2.6}$$

with ε and μ_0 denoting the time domain permittivity of the host medium and permeability in a vacuum in F/m and H/m, respectively.

Noting that

$$\varepsilon(\vec{r}, t) = \varepsilon_0[\delta(t) + \chi(\vec{r}, t)], \tag{2.7}$$

with ε_0 denoting the permittivity in a vacuum in F/m and χ the dimensionless time-domain susceptibility of the host medium, equation (2.5) can also be written as

$$\vec{D}(\vec{r}, t) = \varepsilon_0 \int_{-\infty}^{t} \left[\delta(t-\tau) + \chi(\vec{r}, t-\tau)\right] \vec{E}(\vec{r}, \tau)\mathrm{d}\tau = \varepsilon_0\vec{E}(\vec{r}, t) + \vec{P}(\vec{r}, t), \tag{2.8}$$

where the induced polarization of the host medium in $\mathrm{C/m^2}$ is defined as

$$\vec{P}(\vec{r}, t) \equiv \varepsilon_0 \int_{-\infty}^{t} \chi(\vec{r}, t-\tau)\vec{E}(\vec{r}, \tau)\mathrm{d}\tau. \tag{2.9}$$

For an electromagnetic field at optical frequencies

$$\rho = 0. \tag{2.10}$$

In a passive area without any radiative recombination process

$$\vec{J} = 0. \tag{2.11}$$

In an active area with a spontaneous emission process

$$\vec{J} = \vec{J}_{\mathrm{sp}}. \tag{2.12}$$

It is worth mentioning that, in an active area, the stimulated emission process will be included in the susceptibility, as it is a purely homogeneous process induced by a given electric field. Therefore, the stimulated emission process is excluded from equation (2.12), as the driven current must be a purely inhomogeneous source.

By using equations (2.5) and (2.6), the electrical and magnetic flux densities $\vec{D}$ and $\vec{B}$ can be eliminated from equations (2.1) and (2.2); hence we obtain

$$\nabla \times \vec{E} = -\mu_0 \frac{\partial}{\partial t}\vec{H}, \tag{2.13}$$

$$\nabla \times \vec{H} = \varepsilon_0 \frac{\partial}{\partial t}\vec{E} + \frac{\partial}{\partial t}\vec{P} + \vec{J}_{\mathrm{sp}}. \tag{2.14}$$

At least in principle, equations (2.13), (2.14) and (2.9) can be solved directly under the given semiconductor material property described by the susceptibility χ over the entire device structure and the spontaneous emission source $\vec{J}_{\mathrm{sp}}$ in the active area. For example, a finite difference time domain (FDTD) approach can be used to discretize equations (2.13) and (2.14) on Yee's unit cells [1]. Each electrical and magnetic field component can therefore be solved through the resulted recursion in the time domain on those cells that fill out the whole device domain. However, although FDTD based numerical solvers have been very successful in dealing with passive structures, they have seldom been employed for solving active structures because of the highly dispersive material property with embedded non-linearity and distributed inhomogeneous driving source. Moreover, every component of the electrical and magnetic fields must be handled as an unknown variable, which exhausts memory capacity and hence makes the computation impossible for devices with sizeable domains. For this reason, a wave equation model with a reduced number of unknown variables is usually more convenient in dealing with active devices.

2.1.2 The wave equation

The duality principle implies that it is not necessary to use both electrical and magnetic fields to describe optical wave propagation: either an electrical or magnetic field will be sufficient. To reduce the number of variables involved, we perform $\nabla\times$ on both sides of equation (2.13) and replace the right hand side (RHS) $\nabla \times \vec{H}$ with equation (2.14) to obtain

$$\nabla(\nabla \cdot \vec{E}) - \nabla^2 \vec{E} = -\mu_0 \left(\varepsilon_0 \frac{\partial^2}{\partial t^2} \vec{E} + \frac{\partial^2}{\partial t^2} \vec{P} + \frac{\partial}{\partial t} \vec{J}_{\mathrm{sp}} \right). \tag{2.15}$$

From equations (2.3), (2.8), (2.10) and (2.9), we also have

$$\begin{aligned}\nabla \cdot \vec{E} &= -\frac{1}{\varepsilon_0} \nabla \cdot \vec{P} = -\int_{-\infty}^{t} \nabla \cdot \left[\chi(\vec{r}, t-\tau) \vec{E}(\vec{r}, \tau) \right] \mathrm{d}\tau \\ &= -\int_{-\infty}^{t} \chi(\vec{r}, t-\tau) \left[\nabla \cdot \vec{E}(\vec{r}, \tau) \right] \mathrm{d}\tau - \int_{-\infty}^{t} \left[\nabla \chi(\vec{r}, t-\tau) \cdot \vec{E}(\vec{r}, \tau) \right] \mathrm{d}\tau.\end{aligned} \tag{2.16}$$

If we restrict our model to those structures with

$$\nabla \chi(\vec{r}, t) \cdot \vec{E}(\vec{r}, t) \approx 0, \tag{2.17}$$

we find

$$\nabla \cdot \vec{E} = 0. \tag{2.18}$$

Hence equation (2.15) becomes

$$\nabla^2 \vec{E} = \frac{1}{\mathrm{c}^2} \frac{\partial^2}{\partial t^2} \vec{E} + \frac{1}{\mathrm{c}^2 \varepsilon_0} \frac{\partial^2}{\partial t^2} \vec{P} + \mu_0 \frac{\partial}{\partial t} \vec{J}_{\mathrm{sp}}, \tag{2.19}$$

with

$$\mathrm{c} \equiv 1/\sqrt{(\mu_0 \varepsilon_0)}, \tag{2.20}$$

defined as the speed of light in a vacuum in m/s.

Condition (2.17) holds for those structures with weak optical guidance, i.e., χ only changes slightly in the plane perpendicular to the wave propagation direction, as such $\nabla_{\mathrm{T}} \chi(\vec{r}, t) \cdot \vec{E}_{\mathrm{T}}(\vec{r}, t) \approx 0$. Along the wave propagation direction (assumed to be z), however, $\partial \chi / \partial z$ does not need to be small since $E_z \approx 0$ anyway. Therefore, wave equation (2.19) holds even for devices with non-uniform structures along the wave propagation direction, e.g., distributed feedback (DFB) or distributed Bragg reflector (DBR) lasers, as long as the wave is weakly guided in the cross-section.

Expressions (2.19) and (2.9) form the wave equation model that describes optical wave propagation in a weakly guided device structure. In the wave equation (2.19), the only term on the left hand side (LHS) gives the spatial diffraction of the electrical field, while the first term on the RHS gives the time dispersion of the electrical field. The balance of these two terms gives the inherent property of the optical wave, i.e., the propagation in space. The second term on the RHS denotes the contribution from the wave–media interaction where the convolution reveals that the wave at a certain time t will be affected by the whole past "history" of the media response. This is simply because the media cannot instantaneously respond to the incident wave. The last term on the RHS represents the contribution of the spontaneous emission known as a noise current source. As the only inhomogeneous term, it plays a crucial role as the "seed" in light-emitting devices. Without the inclusion of this inhomogeneous contribution in equation (2.19), a laser will never lase as equation (2.19) would have only zero solution because of its homogeneity.

In comparison with the Maxwell equations in their original form, the wave equation model is physically straightforward and has minimum required unknown variables involved. However, equation (2.19) contains the second order derivatives with respect to time and is in the form of a hyperbolic partial differential equation (PDE). Unlike an elliptical PDE with only static solutions, or a parabolic PDE with solutions exponentially approaching its steady state, a hyperbolic PDE takes harmonic oscillations as its inherent solution and bears no time-invariant steady state. Therefore, stability will always be an issue in looking for its solutions if the initial value is not well posed or not sufficiently smooth.

Knowing that a hyperbolic PDE takes the harmonic wave as its "static" solution, we can therefore write the general solution of the wave equation (2.19) in the form of a "modulated" wave, i.e., a harmonic wave with "slow-varying" envelope. By doing so, we should be able to extract a governing equation for this envelope from equation (2.19). As the envelope changes more slowly, the new equation will take a reduced time derivative and hence become more stable.

2.2 The reduced wave equation in the time domain

We assume that the optical wave is composed of harmonic waves with discrete frequencies and relatively slow-varying envelopes

$$\vec{E}(\vec{r},t) = \frac{1}{2}\sum_k \vec{u}_k(\vec{r},t)\mathrm{e}^{-\mathrm{j}\omega_k t} + \text{c.c.}, \tag{2.21}$$

with $\vec{u}_k$ and ω_k indicating the kth harmonic wave envelope function in V/m and angular frequency in rad/s, respectively, and where c.c. means complex conjugate. By further assuming the linearity of equation (2.19) (i.e., χ has no explicit dependence on $\vec{E}$), we take only a single frequency ($k = 0$) in the following derivations without losing generality: when multiple frequencies are involved, it is trivial to consider a summation in a linear system because of the superposition principle. For the same reason, we can drop the complex conjugate part by considering

$$\vec{E}(\vec{r},t) = \vec{u}(\vec{r},t)\mathrm{e}^{-\mathrm{j}\omega_0 t}, \tag{2.22}$$

only, with ω_0 as the harmonic wave frequency (or reference frequency) and with the subscript of the envelope function omitted. Since equations (2.19) and (2.9) are all real, if we take our real-world optical wave as the real (or imaginary) part of equation (2.22), our real-world result will then be the real (or imaginary) part of the solution obtained from equations (2.19) and (2.9). The reason that we use a complex exponential function to replace the sinusoidal function is that the former is the eigenfunction of any linear and time-invariant system, whereas the latter is not, unless it forms a proper linear combination, i.e., a complex exponential function.

Replacing the optical field in equation (2.9) with equation (2.22) yields

$$\begin{aligned}\vec{P}(\vec{r},t) &= \varepsilon_0 \int_{-\infty}^{t} \chi(\vec{r},t-\tau)\vec{u}(\vec{r},\tau)\mathrm{e}^{-\mathrm{j}\omega_0\tau}\,\mathrm{d}\tau = \varepsilon_0 F^{-1}\left[\widetilde{\chi}(\vec{r},\omega)\widetilde{\vec{u}}(\vec{r},\omega-\omega_0)\right] \\ &\approx \varepsilon_0\widetilde{\chi}(\vec{r},\omega_0)F^{-1}\left[\widetilde{\vec{u}}(\vec{r},\omega-\omega_0)\right] = \varepsilon_0\widetilde{\chi}(\vec{r},\omega_0)\vec{u}(\vec{r},t)\mathrm{e}^{-\mathrm{j}\omega_0 t},\end{aligned} \tag{2.23}$$

with $\widetilde{\vec{u}}$ and $\widetilde{\chi}$ indicating the frequency domain responses of the slow-varying harmonic wave envelope function and susceptibility, respectively, and $F^{-1}[\ldots]$ the inverse Fourier transform. Equation (2.23) holds only when the susceptibility varies much faster than the slow-varying envelope in the time domain; or equivalently, the bandwidth of $\widetilde{\chi}$ is much larger than that of $\widetilde{\vec{u}}$ in the frequency domain. In optoelectronic devices, this is usually true as long as the base-band signal (hence the slow-varying envelope) does not consist of very short pulses. Since the full width half maximum (FWHM) bandwidth of $\widetilde{\chi}$ is usually as broad as 5–10 THz (i.e., around 50–100 nm in a C-band centered at 1550 nm), i.e., χ can respond to any time change slower than sub-picosecond, any base-band signal that varies slower than 10 ps would make equation (2.23) a valid approximation.

We now plug both equations (2.22) and (2.23) into equation (2.19) to obtain

$$\mathrm{j}\frac{2\omega_0}{\mathrm{c}^2}\left[1+\widetilde{\chi}(\vec{r},\omega_0)\right]\frac{\partial\vec{u}}{\partial t} = -\nabla^2\vec{u} - \frac{\omega_0^2}{\mathrm{c}^2}\left[1+\widetilde{\chi}(\vec{r},\omega_0)\right]\vec{u} + \mu_0\mathrm{e}^{\mathrm{j}\omega_0 t}\frac{\partial}{\partial t}\vec{J}_{\mathrm{sp}}, \tag{2.24}$$

where under the slow-varying envelope assumption ($|\partial^2\vec{u}/\partial t^2| \ll \omega_0^2|\vec{u}|$), $\partial^2\vec{u}/\partial t^2$ is dropped.

Equation (2.24) is the reduced wave equation in the time domain. It governs the slow-varying envelope of an optical field that is assumed in a harmonic wave form with optical frequency ω_0. Compared with equation (2.19), equation (2.24) has the fast-varying harmonic factor ($\mathrm{e}^{-\mathrm{j}\omega_0 t}$) excluded, hence has a reduced time derivative order. Numerically, stable solutions can be obtained through time domain discretization by following the envelope change ($\partial\vec{u}/\partial t$), rather than by following the optical wave change ($\partial\vec{E}/\partial t$) itself. This normally results in a great saving of progressive steps as the former changes much slower than the latter in the time domain.

Actually, equation (2.24) is solved directly only when the device structure does not have any dominant feature in space and hence the wave does not form any time-invariant spatial pattern known as a "mode." In waveguide based optoelectronic and photonic devices, however, the wave is confined at least along one dimension. Therefore, an optical mode can be introduced at least along this dimension and the wave will travel in the reduced spatial dimensions. For this reason, equation (2.24) can be further simplified for waveguide based optoelectronic and photonic devices as shown in Section 2.4.

2.3 The reduced wave equation in the space domain

Because of the symmetry embedded in wave equation (2.19) in respect of time and space, in principle we can also assume that the optical wave is composed of plane waves with discrete propagation constants and relatively slow-varying envelope functions. More specifically, by assuming that the propagation of these plane waves is all in the z direction, we can write

$$\vec{E}(\vec{r},t) = \frac{1}{2}\sum_k \vec{v}_k(\vec{r},t)\mathrm{e}^{\mathrm{j}\beta_k z} + \text{c.c.}, \tag{2.25}$$

with $\vec{v}_k$ and β_k indicating the kth plane wave envelope function in V/m and propagation constant in rad/m, respectively. In equation (2.25), the envelope function is only slow-varying in z but can change arbitrarily in the perpendicular xy plane. Again, under the linear assumption of equation (2.19), we need only to consider

$$\vec{E}(\vec{r},t) = \vec{v}(\vec{r},t)\mathrm{e}^{\mathrm{j}\beta_0 z}. \tag{2.26}$$

Replacing the optical field in equation (2.9) with equation (2.26) yields

$$\vec{P}(\vec{r},t) = \varepsilon_0 \int_{-\infty}^{t} \chi(\vec{r},t-\tau)\vec{v}(\vec{r},\tau)\mathrm{e}^{\mathrm{j}\beta_0 z}\,\mathrm{d}\tau = \vec{p}(\vec{r},t)\mathrm{e}^{\mathrm{j}\beta_0 z}, \tag{2.27}$$

with the slow-varying polarization envelope function defined as

$$\vec{p}(\vec{r},t) \equiv \varepsilon_0 \int_{-\infty}^{t} \chi(\vec{r},t-\tau)\vec{v}(\vec{r},\tau)\mathrm{d}\tau. \tag{2.28}$$

We now plug both equations (2.26) and (2.27) into equation (2.19) to obtain

$$\frac{\partial^2\vec{v}}{\partial x^2} + \frac{\partial^2\vec{v}}{\partial y^2} + 2\mathrm{j}\beta_0\frac{\partial\vec{v}}{\partial z} = \frac{1}{\mathrm{c}^2}\frac{\partial^2\vec{v}}{\partial t^2} + \frac{1}{\mathrm{c}^2\varepsilon_0}\frac{\partial^2\vec{p}}{\partial t^2} + \beta_0^2\vec{v} + \mu_0\mathrm{e}^{-\mathrm{j}\beta_0 z}\frac{\partial}{\partial t}\vec{J}_{\mathrm{sp}}, \tag{2.29}$$

where under the slow-varying envelope assumption ($|\partial^2\vec{v}/\partial z^2| \ll \beta_0^2|\vec{v}|$), $\partial^2\vec{v}/\partial z^2$ is dropped.

Equation (2.29) is the reduced wave equation in the space domain. Together with equation (2.28), it governs the slow-varying envelope of an optical field which is assumed in a modulated plane wave form with its propagation constant β_0 in the z direction. Compared with equation (2.19), equation (2.29) has the fast-varying phase factor ($\mathrm{e}^{\mathrm{j}\beta_0 z}$) excluded, hence it has a reduced (from second to first) spatial derivative order in at least one of the three dimensions. However, unlike equation (2.24), equation (2.29) is not well posed [2]. Therefore, no finite difference algorithm in the time domain will lead to a stable solution to equation (2.29). For this reason, we do not use equation (2.29) directly but proceed to reduce the time derivative orders following the method in Section 2.2 to make equation (2.29) a well-posed problem.

2.4 The reduced wave equation in both time and space domains – the traveling wave model

In waveguide based optoelectronic and photonic devices, the optical wave usually propagates along one direction and is fully or partially confined in the cross-sectional plane perpendicular to the propagation direction. Either starting from the reduced wave equation in the time domain (2.24) or starting from the reduced wave equation in the space domain (2.29), we can further simplify the optical governing equation under such a condition.

2.4.1 The wave equation in fully confined structures

If the optical wave propagates only along z and is fully confined in the cross-sectional xy plane, and if the waveguide transverse structure is uniform along z, we can write the optical field in equation (2.19) as

$$\vec{E}(\vec{r},t) = \frac{1}{2}\vec{s}\phi(x,y)e(z,t)\mathrm{e}^{\mathrm{j}(\beta_0 z-\omega_0 t)} + \text{c.c.}, \tag{2.30}$$

where

$\vec{s}$ = unit vector along the polarization direction of the optical field $\vec{E}$,
$\phi(x,y)$ = cross-sectional field distribution in 1/m known as the optical mode or the eigenfunction of the optical waveguide,
$e(z,t)$ = longitudinal field envelope function in V taking relatively slow change with time and along the propagation direction,
$\mathrm{e}^{\mathrm{j}(\beta_0 z-\omega_0 t)}$ = dimensionless propagation factor in the form of $f(z-vt)$ known as a (harmonic) plane wave traveling at a phase velocity defined by ω_0/β_0.

Expression (2.30) clearly shows that the optical field is factorized into a fast-varying plane wave traveling along z, which is also modulated by an envelope function with slow variation in z and t, and a fixed mode profile in the cross-sectional area without any change in the z direction.

A typical example of such a structure, known as the ridge waveguide, is illustrated in Fig. 2.1.

Under the linear assumption made in equation (2.19), we can rewrite equation (2.30) as

$$\vec{E}(\vec{r},t) = \vec{x}\phi(x,y)e(z,t)\mathrm{e}^{\mathrm{j}(\beta_0 z-\omega_0 t)}, \tag{2.31}$$

with $\vec{x}$ indicating the unit vector along x. Here we have considered only one polarization direction, taken to be x, without losing generality. Comparing equation (2.31) with equation (2.22), we know that the optical envelope function in equation (2.24) must be in the form

$$\vec{u}(\vec{r},t) = \vec{x}\phi(x,y)e(z,t)\mathrm{e}^{\mathrm{j}\beta_0 z}. \tag{2.32}$$

As a consequence of (2.32), again our final result will be the real part of the solution only.

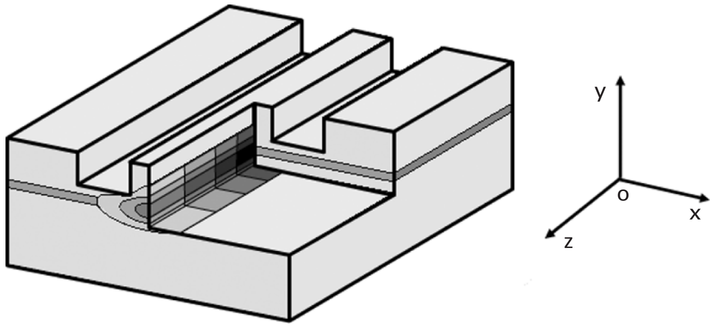

Fig. 2.1. A ridge waveguide structure in which the optical field can be factorized into a modulated plane wave traveling in the z direction and a mode profile in the xy plane without change in z.

Replacing the envelope function in equation (2.24) by expression (2.32), we find:

$$\left\{\mathrm{j}\frac{2k_0}{c}[1+\widetilde{\chi}(\vec{r},\omega_0)]\frac{\partial e(z,t)}{\partial t}+2\mathrm{j}\beta_0\frac{\partial e(z,t)}{\partial z}\right\}\phi(x,y)$$
$$=-e(z,t)\left\{\frac{\partial^2}{\partial x^2}+\frac{\partial^2}{\partial y^2}-\beta_0^2+k_0^2[1+\widetilde{\chi}(\vec{r},\omega_0)]\right\}\phi(x,y)+\mu_0\mathrm{e}^{-\mathrm{j}(\beta_0 z-\omega_0 t)}\frac{\partial J_{\mathrm{sp}x}}{\partial t}, \tag{2.33}$$

where $k_0 \equiv \omega_0/\mathrm{c}$ and $J_{\mathrm{sp}x} \equiv \vec{J}_{\mathrm{sp}} \cdot \vec{x}$. Under the slow-varying envelope assumption ($|\partial^2 e/\partial z^2| \ll |\beta_0|^2|e|$), $\partial^2 e/\partial z^2$ is dropped from equation (2.33). Since the optical field is fully confined in the cross-sectional area with a background material refractive index distribution denoted as $n(x, y, \omega_0)$, we will be able to find the time-invariant optical field distribution in the xy plane, known as the optical mode, by solving the following eigenvalue problem:

$$\left(\frac{\partial^2}{\partial x^2}+\frac{\partial^2}{\partial y^2}\right)\phi(x,y)+k_0^2 n^2(x,y,\omega_0)\phi(x,y)=\beta_0^2\phi(x,y), \tag{2.34}$$

subject to the normalization condition

$$\int_\Sigma \phi^2(x,y)\mathrm{d}x\,\mathrm{d}y=1, \tag{2.35}$$

with Σ indicating the entire cross-sectional area in m^2 where the optical mode spreads.

Substitute the spatial derivative terms in the xy plane in equation (2.33) by equation (2.34), multiply the optical mode $\phi(x, y)$ on both sides of the equation obtained, and integrate over the entire cross-sectional area to yield

$$\frac{1}{n_{\mathrm{eff}}\mathrm{c}}\left\{\int_\Sigma[1+\widetilde{\chi}(\vec{r},\omega_0)]\phi^2(x,y)\mathrm{d}x\,\mathrm{d}y\right\}\frac{\partial e(z,t)}{\partial t}+\frac{\partial e(z,t)}{\partial z}$$
$$=\mathrm{j}\frac{k_0}{2n_{\mathrm{eff}}}\left\{\int_\Sigma[1+\widetilde{\chi}(\vec{r},\omega_0)-n^2(x,y,\omega_0)]\phi^2(x,y)\mathrm{d}x\,\mathrm{d}y\right\}e(z,t)+\widetilde{s}(z,t), \tag{2.36}$$

where the inhomogeneous spontaneous emission contribution in V/m is given as

$$\widetilde{s}(z,t) \equiv -\frac{\mathrm{j}e^{-\mathrm{j}(\beta_0 z-\omega_0 t)}}{2n_{\mathrm{eff}}\omega_0}\sqrt{\left(\frac{\mu_0}{\varepsilon_0}\right)}\int_\Sigma \frac{\partial J_{\mathrm{spx}}}{\partial t}\phi(x,y)\mathrm{d}x\,\mathrm{d}y, \tag{2.37}$$

with the dimensionless effective index defined as $n_{\mathrm{eff}} \equiv \beta_0/k_0$.

In optoelectronic and photonic devices with full wave confinement in the cross-sectional area, external bias is usually applied along the wave propagation direction in z, which introduces a material gain and an associated refractive index change inside the active region along this direction. Noting that the material gain per wavelength cycle (i.e., $g/k_0 = gc/\omega_0 = g\lambda_0/2\pi$, with λ_0 denoting the reference wavelength in a vacuum) and the refractive index change (i.e., Δn), both induced by the external bias, appear to be much smaller than the background (i.e., under zero external bias or “cold cavity”) material refractive index $n(x,y,\omega_0)$, which is uniform along z, we find

$$\begin{aligned} n^2(\vec{r},\omega_0) &= [n(x,y,\omega_0)+\Delta n(z,\omega_0)]^2 \\ &\approx n^2(x,y,\omega_0)+2n(x,y,\omega_0)\Delta n(z,\omega_0), \end{aligned} \tag{2.38}$$

$$g(\vec{r},\omega_0) = g(z,\omega_0)-\alpha(x,y,z), \tag{2.39}$$

$$\begin{aligned} 1+\widetilde{\chi}(\vec{r},\omega_0) &= \left[n(\vec{r},\omega_0)-\frac{\mathrm{j}}{2k_0}g(\vec{r},\omega_0)\right]^2 \\ &\approx n^2(x,y,\omega_0)+2n(x,y,\omega_0)\Delta n(z,\omega_0)-\frac{\mathrm{j}}{k_0}n(x,y,\omega_0)[g(z,\omega_0)-\alpha(x,y,z)]. \end{aligned} \tag{2.40}$$

In equations (2.38) to (2.40), we have defined the following:

$n(\vec{r},\omega_0)$ = dimensionless material refractive index,
$n(x,y,\omega_0)$ = dimensionless cross-sectional area refractive index under zero bias, also known as the background or “cold cavity” refractive index,
$\Delta n(z,\omega_0)$ = dimensionless bias induced refractive index change, non-zero only inside the active region,
$g(\vec{r},\omega_0)$ = material gain in 1/m,
$g(z,\omega_0)$ = bias induced interband stimulated emission gain (or loss, when it is negative) in 1/m, non-zero only inside the active region,
$\alpha(x,y,z)$ = optical loss in 1/m because of non-interband processes such as free-carrier absorption and scattering.

We have also dropped higher order terms such as $(\Delta n)^2$, $(g/k_0)^2$ and $(\Delta n)(g/k_0)$.

By utilizing equation (2.40) and noting that the interband stimulated emission gain $g(z,\omega_0)$ and the associated refractive index change $\Delta n(z,\omega_0)$ exist only inside the active region, we can derive

$$\int_\Sigma [1+\widetilde{\chi}(\vec{r},\omega_0)]\phi^2(x,y)\mathrm{d}x\,\mathrm{d}y \approx \int_\Sigma n^2(x,y,\omega_0)\phi^2(x,y)\mathrm{d}x\,\mathrm{d}y \equiv \overline{n}^2 \tag{2.41a}$$

and

$$
\begin{aligned}
&\int_{\Sigma} [1 + \widetilde{\chi}(\vec{r}, \omega_0) - n^2(x, y, \omega_0)]\phi^2(x, y)\mathrm{d}x\, \mathrm{d}y \\
&\quad \approx \left[2\Delta n(z, \omega_0) - \frac{\mathrm{j}}{k_0} g(z, \omega_0)\right] \int_{\Sigma_{\mathrm{ar}}} n(x, y, \omega_0)\phi^2(x, y)\mathrm{d}x\, \mathrm{d}y \\
&\qquad + \frac{\mathrm{j}}{k_0} \int_{\Sigma} n(x, y, \omega_0)\alpha(x, y, z)\phi^2(x, y)\mathrm{d}x\, \mathrm{d}y \\
&\quad \approx \overline{n}\Gamma \left[2\Delta n(z, \omega_0) - \frac{\mathrm{j}}{k_0} g(z, \omega_0)\right] + \frac{\mathrm{j}}{k_0} \overline{n\alpha}(z),
\end{aligned}
\tag{2.41b}
$$

with Σ_{ar} defined as the cross-sectional area of the active region. Also in deriving equation (2.41b), we have utilized the following approximations:

$$
\int_{\Sigma_{\mathrm{ar}}} n(x, y, \omega_0)\phi^2(x, y)\mathrm{d}x\, \mathrm{d}y \approx \overline{n} \int_{\Sigma_{\mathrm{ar}}} \phi^2(x, y)\mathrm{d}x\, \mathrm{d}y = \overline{n}\Gamma \tag{2.42}
$$

and

$$
\int_{\Sigma} n(x, y, \omega_0)\alpha(x, y, z)\phi^2(x, y)\mathrm{d}x\, \mathrm{d}y \approx \overline{n} \int_{\Sigma} \alpha(x, y, z)\phi^2(x, y)\mathrm{d}x\, \mathrm{d}y = \overline{n\alpha}(z),
\tag{2.43}
$$

with the optical confinement factor and optical modal loss defined as

$$
\Gamma \equiv \frac{\int_{\Sigma_{\mathrm{ar}}} \phi^2(x, y)\mathrm{d}x\, \mathrm{d}y}{\int_{\Sigma} \phi^2(x, y)\mathrm{d}x\, \mathrm{d}y} = \int_{\Sigma_{\mathrm{ar}}} \phi^2(x, y)\mathrm{d}x\, \mathrm{d}y, \tag{2.44}
$$

$$
\overline{\alpha}(z) \equiv \frac{\int_{\Sigma} \alpha(x, y, z)\phi^2(x, y)\mathrm{d}x\, \mathrm{d}y}{\int_{\Sigma} \phi^2(x, y)\mathrm{d}x\, \mathrm{d}y} = \int_{\Sigma} \alpha(x, y, z)\phi^2(x, y)\mathrm{d}x\, \mathrm{d}y. \tag{2.45}
$$

Finally, we plug equations (2.41a) and (2.41b) into equation (2.36) to yield

$$
\frac{1}{v_{\mathrm{g}}} \frac{\partial e(z, t)}{\partial t} + \frac{\partial e(z, t)}{\partial z} = \left[\mathrm{j}k_0\Gamma\Delta n(z, \omega_0) + \frac{1}{2}\Gamma g(z, \omega_0) - \frac{1}{2}\overline{\alpha}(z)\right] e(z, t) + \widetilde{s}(z, t),
\tag{2.46}
$$

where $v_{\mathrm{g}} \equiv \mathrm{c}/n_{\mathrm{g}} \approx \mathrm{c}n_{\mathrm{eff}}/\overline{n}^2$ and $n_{\mathrm{eff}} \approx \overline{n}$ are assumed, and where n_{g} is the group index and v_{g} is the group velocity.

Equation (2.46) governs the envelope function of the optical wave propagating along $+z$. For the optical wave that propagates along the opposite direction $(-z)$, we just need to use $-z$ to replace z in equation (2.46) as both the material property and the spontaneous emission contribution have bidirectional symmetry along $\pm z$. Therefore, we obtain

$$\left(\frac{1}{v_\mathrm{g}}\frac{\partial}{\partial t}+\frac{\partial}{\partial z}\right)e^\mathrm{f}(z,t)=\left[\mathrm{j}k_0\Gamma\Delta n(z,\omega_0)+\frac{1}{2}\Gamma g(z,\omega_0)-\frac{1}{2}\overline{\alpha}(z)\right]e^\mathrm{f}(z,t)+\widetilde{s}^\mathrm{f}(z,t), \tag{2.47a}$$

$$\left(\frac{1}{v_\mathrm{g}}\frac{\partial}{\partial t}-\frac{\partial}{\partial z}\right)e^\mathrm{b}(z,t)=\left[\mathrm{j}k_0\Gamma\Delta n(z,\omega_0)+\frac{1}{2}\Gamma g(z,\omega_0)-\frac{1}{2}\overline{\alpha}(z)\right]e^\mathrm{b}(z,t)+\widetilde{s}^\mathrm{b}(z,t), \tag{2.47b}$$

where we have used the superscripts f and b to indicate the forward and backward propagating wave envelope functions, respectively. In equation (2.47), because the inhomogeneous spontaneous emission contributes to both the forward and backward propagating waves, we have $\widetilde{s}^\mathrm{b}(z,t)=\widetilde{s}^\mathrm{f}(-z,t)$ with $\widetilde{s}^\mathrm{f}$ given by equation (2.37).

The one-dimensional (1D) slow-varying envelope equation (2.47) along the wave propagation direction (i.e., $\pm z$), together with the two-dimensional (2D) eigenvalue equation (2.34) in the cross-sectional area (i.e., the xy plane), form the governing equations for modeling the optical wave that propagates along $\pm z$ and is fully confined by the waveguide in the cross-sectional xy plane. These equations can be solved subject to certain initial and boundary conditions. Since the initial and boundary conditions are related to the operating conditions and structures of specific devices, we will find the effect of these conditions on device performance through examples in Chapter 10.

Once the optical mode $\phi(x,y)$, the forward (along $+z$) and the backward (along $-z$) slow-varying envelopes $e^\mathrm{f}(z,t)$ and $e^\mathrm{b}(z,t)$ are solved by equations (2.34) and (2.47), respectively, the real-world optical field is obtained by using

$$\vec{E}(\vec{r},t)=\frac{1}{2}\vec{x}\phi(x,y)[e^\mathrm{f}(z,t)\mathrm{e}^{\mathrm{j}\beta_0 z}+e^\mathrm{b}(z,t)\mathrm{e}^{-\mathrm{j}\beta_0 z}]\mathrm{e}^{-\mathrm{j}\omega_0 t}+\mathrm{c.c.} \tag{2.48}$$

As seen in the derivation process, we find that this model is valid under the following conditions.

(1) Assumptions on the optical wave.
- Wave propagates along the device in a longitudinal direction only.
- Wave is fully confined in the cross-sectional area perpendicular to the propagation direction.
- Wave has discrete optical frequencies with relatively slow-varying envelopes.

(2) Assumptions on the material.
- Material has linear optical property.
- Material takes no time to respond to any variation of optical wave envelope.

Also, in the above derivations, we have assumed that the optical wave has:

- a single operating frequency (i.e., ω_0);
- a single optical mode (i.e., the waveguide supports a single guided mode only);
- a single polarization state (assumed to be along x).

However, equations (2.34) and (2.47) can readily be expanded to model the optical wave with multiple operating frequencies, or multiple modes, or arbitrary polarization states, by utilizing the linear superposition theory and the mode orthogonality. Therefore, the last three constraints are removable.

By comparing equation (2.31) with equation (2.26), we find that the optical envelope function in equation (2.29) can be written as

$$\vec{v}(\vec{r}, t) = \vec{x}\phi(x, y)e(z, t)\mathrm{e}^{-\mathrm{j}\omega_0 t}. \tag{2.49}$$

Inserting equation (2.32) into equation (2.23) yields

$$\vec{P}(\vec{r}, t) = \vec{x}\varepsilon_0\widetilde{\chi}(\vec{r}, \omega_0)\phi(x, y)e(z, t)\mathrm{e}^{\mathrm{j}(\beta_0 z - \omega_0 t)}. \tag{2.50}$$

Further, comparing equation (2.50) with equation (2.27), we also find

$$\vec{p}(\vec{r}, t) = \vec{x}\varepsilon_0\widetilde{\chi}(\vec{r}, \omega_0)\phi(x, y)e(z, t)\mathrm{e}^{-\mathrm{j}\omega_0 t}. \tag{2.51}$$

By replacing the optical field and polarization envelope functions in equation (2.29) by expressions (2.49) and (2.51), respectively, and utilizing equations (2.34) and (2.35), we obtain equation (2.36) again, as it should be. This confirms that equation (2.47) is the reduced wave equation both in time and space domains; it can be obtained from the full wave equation (2.19) by reducing the time derivative and the space derivative in either sequence. The condition under which the time derivative can be reduced requires the optical field to take an amplitude-modulated harmonic wave in the time domain, with its modulation bandwidth (i.e., the base bandwidth) much smaller than the harmonic wave frequency (i.e., the carrier frequency), as required by the time slow-varying envelope assumption. The condition under which the spatial derivative can be reduced in a certain direction requires the optical field to take an amplitude-modulated plane wave in that direction, with its modulation bandwidth (i.e., the maximum spatial frequency) much smaller than the propagation constant, as required by the spatial slow-varying envelope assumption. Since equation (2.47) has been derived under both conditions, it governs the (slow-varying) envelope function of an optical field in the form of a modulated harmonic plane wave in a certain direction (along z in this derivation). A harmonic plane wave in a certain direction describes a plane wave propagating along that direction. Therefore, equation (2.47) governs the (slow-varying) envelope functions of the two traveling plane waves along $\pm z$, respectively.

2.4.2 The wave equation in partially confined structures

In some applications, the waveguide transverse structure is not uniform along the wave propagation direction. A typical example is a horizontally varied structure such as the horn waveguide [3] shown in Fig. 2.2.

In such a structure, the optical wave is confined only in the vertical direction y, rather than in the entire cross-sectional xy plane. Therefore, instead of equation (2.31), we have

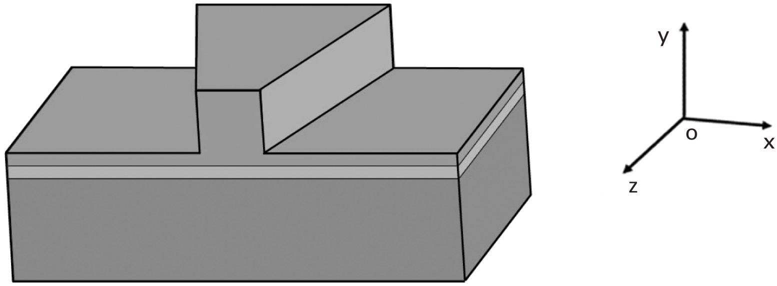

Fig. 2.2. A horn waveguide structure in which the optical wave is confined only in the y direction and is propagating along both z and x directions.

to write the optical field in the form of [4]

$$\vec{E}(\vec{r}, t) = \vec{x}\phi(y)e(x, z, t)\mathrm{e}^{\mathrm{j}(\beta_0 z - \omega_0 t)}, \tag{2.52}$$

with $\phi(y)$ indicating the optical field distribution (or the 1D optical mode) along y in $1/\mathrm{m}^{1/2}$, and $e(x, z, t)$ the envelope function in $\mathrm{V/m}^{1/2}$. In accordance with equation (2.52), we will use

$$\vec{u}(\vec{r}, t) = \vec{x}\phi(y)e(x, z, t)\mathrm{e}^{\mathrm{j}\beta_0 z}, \tag{2.53}$$

to replace equation (2.32) as well. Plugging (2.53) into (2.24), multiplying the 1D optical mode $\phi(y)$ on both sides of the equation obtained, and integrating along the vertical direction y yields

$$\begin{aligned}
&\frac{1}{n_{\mathrm{eff}} c}\left\{\int_{\Sigma_y}[1+\widetilde{\chi}(\vec{r}, \omega_0)]\phi^2(y)\mathrm{d}y\right\}\frac{\partial e(x, z, t)}{\partial t} + \frac{\partial e(x, z, t)}{\partial z} \\
&\quad = \frac{\mathrm{j}}{2n_{\mathrm{eff}} k_0}\frac{\partial^2 e(x, z, t)}{\partial x^2} + \frac{\mathrm{j}k_0}{2n_{\mathrm{eff}}}\left\{\int_{\Sigma_y}[1+\widetilde{\chi}(\vec{r}, \omega_0) - n^2(y, \omega_0)]\phi^2(y)\mathrm{d}y\right\} \\
&\quad \times e(x, z, t) + \widetilde{s}(x, z, t),
\end{aligned} \tag{2.54}$$

where the 1D optical mode along y can be found by solving the following eigenvalue problem

$$\frac{\partial^2}{\partial y^2}\phi(y) + k_0^2 n^2(y, \omega_0)\phi(y) = \beta_0^2\phi(y), \tag{2.55}$$

subject to the normalization condition

$$\int_{\Sigma_y}\phi^2(y)\mathrm{d}y = 1. \tag{2.56}$$

In expressions (2.54) to (2.56), Σ_y indicates the entire vertical range along y in m where the 1D optical mode spreads. Note that $n(y, \omega_0)$ denotes the dimensionless background or "cold cavity" material refractive index distribution along y. Again, $\partial^2 e/\partial z^2$

is dropped from equation (2.54) under the slow-varying envelope assumption. Finally, in equation (2.54), the inhomogeneous spontaneous emission contribution in $\mathrm{V/m^{3/2}}$ is given as

$$\widetilde{s}(x,z,t) \equiv -\frac{\mathrm{j}e^{-\mathrm{j}(\beta_0 z-\omega_0 t)}}{2n_{\mathrm{eff}}\omega_0}\sqrt{\frac{\mu_0}{\varepsilon_0}}\int_{\Sigma_y}\frac{\partial J_{\mathrm{spx}}}{\partial t}\phi(y)\mathrm{d}y. \tag{2.57}$$

In such a waveguide structure, the active region usually expands to an entire xz plane within one of the vertically stacked layers in the y direction. In accordance with the active region distribution, the external bias is usually applied on the top xz plane, which introduces a material gain and an associated refractive index change inside the active region. Similarly to equations (2.38) to (2.40), by assuming that the bias induced material gain per wavelength cycle and the associated refractive index change are perturbations in the background material refractive index distribution, which is uniform in the xz plane, we find

$$n^2(\vec{r},\omega_0) \approx n^2(y,\omega_0) + 2n(y,\omega_0)\Delta n(x,z,\omega_0), \tag{2.58}$$

$$g(\vec{r},\omega_0) = g(x,z,\omega_0) - \alpha(x,y,z), \tag{2.59}$$

$$\begin{aligned}1+\widetilde{\chi}(\vec{r},\omega_0) &= \left[n(\vec{r},\omega_0) - \frac{\mathrm{j}}{2k_0}g(\vec{r},\omega_0)\right]^2 \\ &\approx n^2(y,\omega_0) + 2n(y,\omega_0)\Delta n(x,z,\omega_0) - \frac{\mathrm{j}}{k_0}n(y,\omega_0)\left[g(x,z,\omega_0) - \alpha(x,y,z)\right].\end{aligned} \tag{2.60}$$

In equations (2.58) to (2.60), we have dropped the higher order terms $(\Delta n)^2$, $(g/k_0)^2$ and $(\Delta n)(g/k_0)$.

By utilizing equation (2.60) and noting that the interband stimulated emission gain $g(x,z,\omega_0)$ and the associated refractive index change $\Delta n(x,z,\omega_0)$ exist only inside the active region, we can further derive

$$\int_{\Sigma_y}[1+\widetilde{\chi}(\vec{r},\omega_0)]\phi^2(y)\mathrm{d}y \approx \int_{\Sigma_y} n^2(y,\omega_0)\phi^2(y)\mathrm{d}y \equiv \overline{n}^2 \tag{2.61a}$$

and

$$\begin{aligned}&\int_{\Sigma_y}\left[1+\widetilde{\chi}(\vec{r},\omega_0) - n^2(y,\omega_0)\right]\phi^2(y)\mathrm{d}y \\ &\approx \left[2\Delta n(x,z,\omega_0) - \frac{\mathrm{j}}{k_0}g(x,z,\omega_0)\right]\int_{\Sigma_{\mathrm{ar}y}} n(y,\omega_0)\phi^2(y)\mathrm{d}y \\ &\quad + \frac{\mathrm{j}}{k_0}\int_{\Sigma_y} n(y,\omega_0)\alpha(x,y,z)\phi^2(y)\mathrm{d}y \\ &\approx \overline{n}\Gamma\left[2\Delta n(x,z,\omega_0) - \frac{\mathrm{j}}{k_0}g(x,z,\omega_0)\right] + \frac{\mathrm{j}}{k_0}\overline{n\alpha}(x,z),\end{aligned} \tag{2.61b}$$

with $\Sigma_{\mathrm{ar}y}$ defined as the active region vertical thickness along y. In deriving (2.61b), we have utilized the following approximations:

$$\int_{\Sigma_{\mathrm{ar}y}} n(y,\omega_0)\phi^2(y)\mathrm{d}y \approx \overline{n}\int_{\Sigma_{\mathrm{ar}y}} \phi^2(y)\mathrm{d}y = \overline{n}\Gamma, \tag{2.62}$$

$$\int_{\Sigma_y} n(y,\omega_0)\alpha(x,y,z)\phi^2(y)\mathrm{d}y \approx \overline{n}\int_{\Sigma_y} \alpha(x,y,z)\phi^2(y)\mathrm{d}y = \overline{n}\,\overline{\alpha}(x,z), \tag{2.63}$$

with the optical confinement factor and optical modal loss defined as

$$\Gamma \equiv \frac{\int_{\Sigma_{\mathrm{ar}y}} \phi^2(y)\mathrm{d}y}{\int_{\Sigma_y} \phi^2(y)\mathrm{d}y} = \int_{\Sigma_{\mathrm{ar}y}} \phi^2(y)\mathrm{d}y, \tag{2.64}$$

$$\overline{\alpha}(x,z) \equiv \frac{\int_{\Sigma_y} \alpha(x,y,z)\phi^2(y)\mathrm{d}y}{\int_{\Sigma_y} \phi^2(y)\mathrm{d}y} = \int_{\Sigma_y} \alpha(x,y,z)\phi^2(y)\mathrm{d}y. \tag{2.65}$$

Finally, we plug equations (2.61a) and (2.61b) into equation (2.54) to yield

$$\begin{aligned}\frac{1}{v_{\mathrm{g}}}\frac{\partial e(x,z,t)}{\partial t} + \frac{\partial e(x,z,t)}{\partial z} &= \frac{\mathrm{j}}{2n_{\mathrm{eff}}k_0}\frac{\partial^2 e(x,z,t)}{\partial x^2}\\ &+ \left[\mathrm{j}k_0\Gamma\Delta n(x,z,\omega_0) + \frac{1}{2}\Gamma g(x,z,\omega_0) - \frac{1}{2}\overline{\alpha}(x,z)\right]e(x,z,t) + \widetilde{s}(x,z,t),\end{aligned} \tag{2.66}$$

where again $v_{\mathrm{g}} \equiv \mathrm{c}/n_{\mathrm{g}} \approx \mathrm{c}n_{\mathrm{eff}}/\overline{n}^2$ and $n_{\mathrm{eff}} \approx \overline{n}$ are assumed.

Equation (2.66) governs the envelope function of the optical wave propagating along $+z$. For the optical wave that propagates along the opposite direction ($-z$), we just need to use $-z$ to replace z in equation (2.66) because of the material bidirectional symmetry along $\pm z$. Therefore, we obtain

$$\begin{aligned}\left(\frac{1}{v_{\mathrm{g}}}\frac{\partial}{\partial t} + \frac{\partial}{\partial z}\right)e^{\mathrm{f}}(x,z,t) &= \frac{\mathrm{j}}{2n_{\mathrm{eff}}k_0}\frac{\partial^2}{\partial x^2}e^{\mathrm{f}}(x,z,t)\\ &+ \left[\mathrm{j}k_0\Gamma\Delta n(x,z,\omega_0) + \frac{1}{2}\Gamma g(x,z,\omega_0) - \frac{1}{2}\overline{\alpha}(x,z)\right]e^{\mathrm{f}}(x,z,t) + \widetilde{s}^{\mathrm{f}}(x,z,t),\end{aligned} \tag{2.67a}$$

$$\begin{aligned}\left(\frac{1}{v_{\mathrm{g}}}\frac{\partial}{\partial t} - \frac{\partial}{\partial z}\right)e^{\mathrm{b}}(x,z,t) &= \frac{\mathrm{j}}{2n_{\mathrm{eff}}k_0}\frac{\partial^2}{\partial x^2}e^{\mathrm{b}}(x,z,t)\\ &+ \left[\mathrm{j}k_0\Gamma\Delta n(x,z,\omega_0) + \frac{1}{2}\Gamma g(x,z,\omega_0) - \frac{1}{2}\overline{\alpha}(x,z)\right]e^{\mathrm{b}}(x,z,t) + \widetilde{s}^{\mathrm{b}}(x,z,t),\end{aligned} \tag{2.67b}$$

where again the superscripts f and b distinguish the forward and backward propagating wave envelope functions, and the inhomogeneous spontaneous emission contributions to the forward and backward propagating waves, with $\widetilde{s}^{\mathrm{f}}$ given by equation (2.57) and $\widetilde{s}^{\mathrm{b}}(x,z,t) = \widetilde{s}^{\mathrm{f}}(x,-z,t)$, respectively.

Therefore, the 2D slow-varying envelope equation (2.67) in the xz plane, together with the 1D eigenvalue equation (2.55) in y, form the governing equations for modeling the partially confined (along the vertical direction y) optical wave propagation along $\pm z$. Because of the lack of lateral confinement (in the x direction), the 2D envelope function diffracts laterally as indicated by an extra second-order derivative term in respect of x in the governing equation (2.67). Therefore, as the solution of equation (2.67), the envelope function changes only slowly with z and t, which indicates the wave propagation along $\pm z$; its change in x, however, will be determined by the boundary conditions imposed in the x direction, which is normally related to the device lateral structure, and its rate of change may not slow. Again, equations (2.67) and (2.55) can be solved, once the initial and boundary conditions are specified for a given device.

Finally, the real-world optical field is obtained using

$$\vec{E}(\vec{r}, t) = \frac{1}{2}\vec{x}\phi(y)[e^{\mathrm{f}}(x, z, t)\mathrm{e}^{\mathrm{j}\beta_0 z} + e^{\mathrm{b}}(x, z, t)\mathrm{e}^{-\mathrm{j}\beta_0 z}]\mathrm{e}^{-\mathrm{j}\omega_0 t} + \mathrm{c.c.} \tag{2.68}$$

2.4.3 The wave equation in periodically corrugated structures

In DFB or DBR lasers and other grating based devices, periodically corrugated structures must be employed to provide distributed reflections along with the waveguide. A typical example of such a periodically corrugated waveguide structure is shown in Fig. 2.3.

Unlike the previous structures, in which the forward and backward propagating waves have no interaction until they reach the waveguide ends, such a waveguide allows the forward and backward waves to couple to each other as they propagate through the periodically perturbed structure along the waveguide. Moreover, a periodic structure with period Λ can be expanded as a summation of many harmonic grating orders with their wave numbers ranking as $m2\pi/\Lambda$, where $m = 0, \pm 1, \pm 2, \ldots, \pm\infty$. Assuming that the grating harmonic component in the Mth ($M \geq 1$) order couples the forward and backward propagation waves along the waveguide direction ($\pm z$), the mth ($m > M$) order components will fast decay and hence are negligible. The mth ($m < M$) order components will, however, couple the forward and backward propagating waves to the radiation waves which leave the waveguide at a certain angle to the propagation direction along $\pm z$ [5, 6, 7].

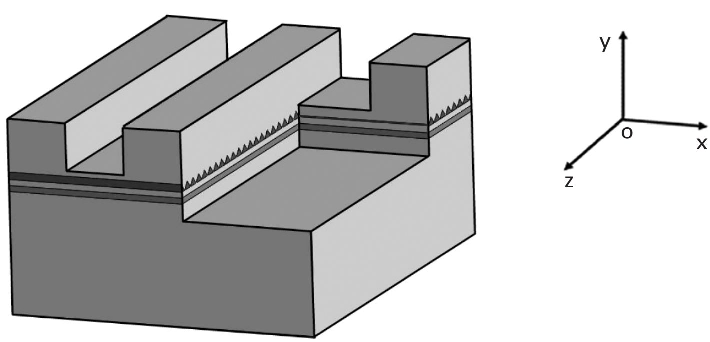

Fig. 2.3. A periodically corrugated waveguide structure in which the propagating waves along $\pm z$ are distributively coupled because of the reflections of the grating.

Since the Mth harmonic order of the grating wave number couples the forward and backward propagation constants, we must have

$$2\delta = \beta_0 - \left(M\frac{2\pi}{\Lambda} - \beta_0\right) = 2\left(\beta_0 - \frac{M\pi}{\Lambda}\right) \ll 2\beta_0, \tag{2.69}$$

where 2δ is the difference of the propagation constants between the original forward and the backward coupled to forward (through the grating backward scattering) propagating waves. Note that -2δ, on the other hand, is the difference in the propagation constants between the original backward and the forward coupled to backward (again through the grating backward scattering) propagating waves. A necessary condition for the forward (and the backward) propagating wave to be sustainable inside the waveguide is apparently that the two forward (and the two backward) propagating wave components have the same propagation constants, known as phase matching. For passive waveguides, we immediately find that the phase matching condition arises at $\delta = 0$. In active waveguides, however, the component with the fastest growing amplitude (because of the gain) does not necessarily correspond to $\delta = 0$. Therefore, the active waveguide may allow sustainable forward and backward propagating waves to have their propagation constants detuned from $\pm M\pi/\Lambda$ (i.e., the Bragg condition), or $\delta \neq 0$. On the scale of β_0 (or π/Λ), the detuning (δ) must be very small, i.e., $\delta/\beta_0 \ll 1$, as otherwise the amplitude loss because of the phase mismatch cannot be compensated for by the amplitude growth from the gain. Therefore, waves with large detuned propagation constants away from the Bragg condition cannot exist. Equation (2.69) addresses such a quasi-phase matching condition in active waveguides.

In accordance with the phase matching condition, we can take the propagation constants of the forward and backward propagating waves as $\pm M\pi/\Lambda$ instead of the previous $\pm\beta_0$ to facilitate deriving the coupled wave equations shown below. However, it is worth mentioning that, by taking $\pm\beta_0$ as the propagation constants of the forward and backward propagating waves in decomposing the total optical field (2.71), we can also get a consistent result.

Also, from the phase matching condition, coupling between the forward and backward propagating waves with propagation constant $\pm M\pi/\Lambda$ and the radiation waves with propagation constant β_r can only happen at

$$\beta_r = \pm\left(\frac{M\pi}{\Lambda} - m\frac{2\pi}{\Lambda}\right) = \pm\frac{M - 2m}{\Lambda}\pi, \tag{2.70a}$$

with $m = 1, 2, 3, \ldots, M/2$ for even M and $m = 1, 2, 3, \ldots, (M-1)/2$ for odd M, respectively. Equation (2.70a) can also be written as

$$\beta_r = \frac{M - 2m}{\Lambda}\pi, \tag{2.70b}$$

with $m = 1, 2, 3, \ldots, M - 1$.

Therefore, in periodically corrugated waveguide structures, we have to retain both forward and backward propagating waves, as well as all the radiation waves that satisfy the phase matching conditions, in decomposing the optical field for deriving the reduced wave equation in both time and space domains. For this reason, we plug

$$\vec{u}(\vec{r},t) = \vec{x}\left\{\phi(x,y)\left[e^{\mathrm{f}}(z,t)\mathrm{e}^{\mathrm{j}\frac{M\pi}{\Lambda}z} + e^{\mathrm{b}}(z,t)\mathrm{e}^{-\mathrm{j}\frac{M\pi}{\Lambda}z}\right] + \sum_{m=1}^{M-1}\hat{e}_m(x,y)\mathrm{e}^{\mathrm{j}\frac{M-2m}{\Lambda}\pi z}\right\}, \tag{2.71}$$

into (2.24) to obtain

$$\begin{aligned}
&\frac{1+\widetilde{\chi}}{n_{\mathrm{eff}}c}\phi\left(\mathrm{e}^{\mathrm{j}\frac{M\pi}{\Lambda}z}\frac{\partial e^{\mathrm{f}}}{\partial t} + \mathrm{e}^{-\mathrm{j}\frac{M\pi}{\Lambda}z}\frac{\partial e^{\mathrm{b}}}{\partial t}\right) + \phi\left(\mathrm{e}^{\mathrm{j}\frac{M\pi}{\Lambda}z}\frac{\partial e^{\mathrm{f}}}{\partial z} - \mathrm{e}^{-\mathrm{j}\frac{M\pi}{\Lambda}z}\frac{\partial e^{\mathrm{b}}}{\partial z}\right) = \\
&\quad \mathrm{j}\frac{1}{2n_{\mathrm{eff}}k_0}\sum_{m=1}^{M-1}\mathrm{e}^{\mathrm{j}\frac{M-2m}{\Lambda}\pi z}\left[\frac{\partial^2}{\partial x^2} + \frac{\partial^2}{\partial y^2} + k_0^2(1+\widetilde{\chi}) - \left(\frac{M-2m}{\Lambda}\right)^2\pi^2\right]\hat{e}_m \\
&\quad + \mathrm{j}\frac{k_0}{2n_{\mathrm{eff}}}\left(1+\widetilde{\chi} - n^2 + \frac{2n_{\mathrm{eff}}\delta}{k_0}\right)\phi\left(e^{\mathrm{f}}\mathrm{e}^{\mathrm{j}\frac{M\pi}{\Lambda}z} + e^{\mathrm{b}}\mathrm{e}^{-\mathrm{j}\frac{M\pi}{\Lambda}z}\right) - \mathrm{j}\frac{\mathrm{e}^{\mathrm{j}\omega_0 t}}{2n_{\mathrm{eff}}\omega_0}\sqrt{\left(\frac{\mu_0}{\varepsilon_0}\right)}\frac{\partial J_{\mathrm{sp}x}}{\partial t},
\end{aligned} \tag{2.72}$$

where equations (2.34) and (2.69) have been used while $\partial^2 e^{\mathrm{f}}/\partial z^2$ and $\partial^2 e^{\mathrm{b}}/\partial z^2$ have been dropped under the slow-varying envelope assumption. Strictly speaking, the radiation wave amplitudes $\hat{e}_m$ should have (z,t) dependence as well, since the forward and backward propagating waves are actually the sources of these radiation waves and the former certainly depends on (z,t). However, as will be seen in equation (2.82), the dependence of $\hat{e}_m$ on (z,t) is implicit (i.e., through e^{f} and e^{b} only), therefore, we can ignore the partial derivatives of $\hat{e}_m$ to (z,t) as the changes of $\hat{e}_m$ on (z,t) are adiabatic. For this reason, we only record $\hat{e}_m$ as explicit functions of (x,y).

Usually the grating itself, i.e., the corrugated part, can be viewed as a perturbation in an optical waveguide with full confinement in the cross-sectional area, which has been discussed in Section 2.4.1 and is known as the unperturbed reference waveguide. Following the change in the grating, the material properties, i.e., the refractive index and gain, all change periodically along the wave propagation direction z. Therefore, we can expand the periodically changed material properties into Fourier series by writing

$$\begin{aligned}
n^2(\vec{r},\omega_0) &= \left[n(x,y,\omega_0) + \sum_{m=-\infty,m\neq 0}^{+\infty}\Delta n_m(x,y)\mathrm{e}^{\mathrm{j}m\frac{2\pi}{\Lambda}z} + \Delta n(z,\omega_0)\right. \\
&\qquad \left. + \sum_{m=-\infty,m\neq 0}^{+\infty}\delta n_m \mathrm{e}^{\mathrm{j}m\frac{2\pi}{\Lambda}z}\right]^2 \\
&\approx n^2(x,y,\omega_0) + 2n(x,y,\omega_0)\Delta n(z,\omega_0) \\
&\quad + 2n(x,y,\omega_0)\sum_{m=-\infty,m\neq 0}^{+\infty}\left[\Delta n_m(x,y) + \delta n_m\right]\mathrm{e}^{\mathrm{j}m\frac{2\pi}{\Lambda}z},
\end{aligned} \tag{2.73}$$

and

$$g(\vec{r},\omega_0) = g(z,\omega_0) + \sum_{m=-\infty,m\neq 0}^{+\infty} \Delta g_m e^{jm\frac{2\pi}{\Lambda}z} - \left[\alpha(x,y,z) + \sum_{m=-\infty,m\neq 0}^{+\infty} \Delta\alpha_m(x,y) e^{jm\frac{2\pi}{\Lambda}z}\right]$$
$$= g(z,\omega_0) - \alpha(x,y,z) + \sum_{m=-\infty,m\neq 0}^{+\infty} [\Delta g_m - \Delta\alpha_m(x,y)]\, e^{jm\frac{2\pi}{\Lambda}z}, \quad (2.74)$$

with Δn_m, δn_m, Δg_m, and $\Delta\alpha_m$ denoting the mth Fourier expansion coefficient of the material refractive index, the (bias induced) index change, the (bias induced) stimulated emission gain, and the optical loss, respectively. In these expansions, the Fourier coefficients are obtained through

$$\Delta n_m(x,y) = \frac{1}{\Lambda}\int_0^\Lambda n_p(x,y,z) e^{-jm\frac{2\pi}{\Lambda}z}\, dz, \quad (2.75a)$$

$$\delta n_m = \frac{1}{\Lambda}\int_0^\Lambda \Delta n_p(z) e^{-jm\frac{2\pi}{\Lambda}z}\, dz, \quad (2.75b)$$

$$\Delta g_m = \frac{1}{\Lambda}\int_0^\Lambda g_p(z) e^{-jm\frac{2\pi}{\Lambda}z}\, dz, \quad (2.75c)$$

$$\Delta\alpha_m(x,y) = \frac{1}{\Lambda}\int_0^\Lambda \alpha_p(x,y,z) e^{-jm\frac{2\pi}{\Lambda}z}\, dz, \quad (2.75d)$$

for $m = 0, \pm 1, \pm 2, \ldots$, with n_p, Δn_p, g_p, and α_p denoting the periodically corrugated part of the material refractive index, the (bias induced) index change, the (bias induced) stimulated emission gain and the optical loss, respectively. Also in equations (2.73) and (2.74), the DC components (i.e., the 0th order coefficients Δn_0, δn_0, Δg_0, and $\Delta\alpha_0$) are merged with their corresponding terms in the reference waveguide where the grating does not exist (i.e., n, Δn, g, and α, respectively). Although it is always possible to select the unperturbed reference waveguide in such a way that the average n_p in one period is equal to zero, hence $\Delta n_0 = 0$, it is generally not possible to have all the DC components disappear for a given corrugated structure, no matter how we select our reference. Therefore, we should not forget to include the DC contribution of the corrugated part to the material properties given in equations (2.73) and (2.74).

From equations (2.73) and (2.74), we can derive

$$1 + \tilde{\chi}(\vec{r},\omega_0) = \left[n(\vec{r},\omega_0) - \frac{j}{2k_0} g(\vec{r},\omega_0)\right]^2$$
$$\approx 1 + \tilde{\chi}_0(\vec{r},\omega_0) + 2n(x,y,\omega_0) \sum_{m=-\infty,m\neq 0}^{+\infty} A_m(x,y) e^{jm\frac{2\pi}{\Lambda}z}, \quad (2.76a)$$

with

$$A_m(x,y) \equiv \Delta n_m(x,y) + \delta n_m - \frac{j}{2k_0}[\Delta g_m - \Delta\alpha_m(x,y)], \quad (2.76b)$$